



# Chapter 3

## A Novel Approach for Plate Impact Experiments to Obtain Properties of Materials Under Extreme Conditions

Bryan Zuanetti, Tianxue Wang, and Vikas Prakash

**Abstract** In this paper we present a novel approach to conduct normal plate impact experiments at elevated temperatures up to 1000 °C. To enable this approach, custom adaptations are made to the breech-end of the single-stage gas-gun at Case Western Reserve University. These adaptations include a precision-machined steel extension piece, which is strategically designed to mate the existing gun-barrel by providing a high tolerance match to the bore and keyway. The extension piece contains a vertical cylindrical heater-well, which houses a resistive coil heater attached to a vertical stem with axial/rotational degrees of freedom. The assembly enables thin metal specimens held at the front-end of a heat-resistant sabot to be heated uniformly across the diameter to the desired test temperatures. Using the configuration, symmetric normal plate impact experiments are conducted on 99.6% tungsten carbide (no binder) using a heated (room temperature to 650 °C) WC flyer plate and a room temperature WC target plate at impact velocities ranging from 233 to 248 m/s. The measured free-surface particle velocity profiles are used to obtain the elastic/plastic behavior of the impacting WC plates as well as the temperature-dependent shock impedance of the flyer. The results indicate a dynamic strength of approximately 6 GPa for the WC used in the present study (strain-rates of about  $10^5$ ), and a decreasing flyer plate longitudinal impedance with increasing temperatures up to 650 °C.

**Keywords** Normal plate impact · Incipient plasticity · Elevated temperatures · Tungsten carbide · Hugoniot elastic limit · Longitudinal impedance

### 3.1 Introduction

It is well understood that dynamic response of most engineering materials is pressure, temperature, and rate sensitive. In this regard, investigations aimed towards exploration of material behavior (i.e. plasticity, strength and failure) at thermomechanical extremes can be experimentally challenging, and thus, knowledge of the dynamic response of materials in certain thermomechanical regimes is still limited by the deficiency of reliable experimental data. Consequently, there is an opportunity for contributions from research in the realm of experimental techniques and novel diagnostics.

Traditionally, light gas-guns and/or explosively driven plate impact experiments have been utilized to study the dynamic inelasticity and other phenomenon such as spallation, or phase transformation that occur with very high strain rates ( $10^5$ – $10^7$ /s), or combinations of high stresses (hydrostatic and/or deviatoric) under dynamic loading conditions [1–3]. These tools have also been adapted to include heating elements which enable investigations of material behavior to extend into thermomechanical extremes. These adaptations usually involve the addition of an induction, or of a resistive heater element to the target-end of the gas-gun [4–6]. Though these adaptations have been shown to be experimentally feasible, the approach inherently leads to special experimental challenges, which require careful considerations. Some of these challenges include: (1) heating the target using an induction coil heating system or a resistive heater, subjects various elements of the target holder and/or the alignment-fixture to differential thermal expansion, requiring remotely controlled alignment adjustment tools with continuous feedback for maintaining parallelism of the target and flyer plates; (2) heating the target plate in combined pressure-shear plate impact configuration requires the fabrication of heat-resistant optical holographic gratings on the target free surface for the measurement of the free surface particle velocity motion during the experiments; (3) a limitation on the stress-states that can be imparted on the sample in certain plate impact configurations that involve sandwiched specimens between hard elastic target plates, because of possible thermal softening of heated target plates that must remain elastic during impact to allow unambiguous interpretation of the experimental results from the measured particle velocity profiles;

---

B. Zuanetti · T. Wang · V. Prakash (✉)

Department of Mechanical and Aerospace Engineering, Case Western Reserve University, Cleveland, OH, USA

e-mail: [vikas.prakash@case.edu](mailto:vikas.prakash@case.edu)

and (4), differential thermal expansion of the target assembly, particularly for targets that utilize an optical window, since precise tolerances between the sample, bond layer, coating(s), and window are difficult to maintain over large temperature ranges [7].

Despite advances in our previous state of understanding regarding the dynamic behavior of materials, significant questions still remain unclear. A few of these important questions are: What is the origin of enhanced strain-rate sensitivity observed in metals? What is the cause for the observed weak thermal softening in metals near their liquid-solidus transition temperature at high loading rates? Will the evolution of dislocation structures continue to play a major role in controlling the shearing resistance of metals near their melting temperature? And, how can existing dynamic plasticity models be updated in order to fully correlate the observed mechanical response of metals over large strain-rate, pressure, and temperature ranges? The objective of the current research is to address some of these important questions by extending the capability of the current plate impact experiments to obtain experimental data under thermomechanical extremes.

The present paper discusses a novel approach for performing elevated temperature plate impact investigations utilizing a breech-end sabot heater system, which enables thin metal specimens held at the front-end of a heat-resistant sabot to be heated to temperatures in excess of 1000 °C, prior to firing, thus allowing high temperature normal and/or combined pressure-shear plate impact experiments to be conducted while alleviating several of the aforementioned experimental challenges. We present results from three normal plate impact elevated temperature experiments conducted on 99.6% pure tungsten carbide (WC), in which the WC flyer plates are heated to temperatures in the range from 23 to 650 °C. The approach enables the Hugoniot Elastic Limit (HEL) of WC, corresponding to its dynamic strength under uniaxial strain, to be obtained, and also estimation of the temperature-dependent longitudinal impedance of the heated WC flyer plate. The results indicate a HEL  $\sim$  6.0 GPa for WC at strain-rates of about  $10^5$ /s, and a decrease in the longitudinal impedance of WC by about 22% as the WC flyer temperatures are increased from 23 to 650 °C.

## 3.2 Experimental Procedure

The schematic of the elevated temperature normal plate impact experiment is shown in Fig. 3.1. To conduct the elevated temperature experiments, the specimen (flyer plate) on the sabot, at the breech end of the gun barrel, is heated by a resistive heater housed in a custom designed extension piece made from SAE 4340 steel. The extension piece (shown in red) is approximately 610 mm in length and contains an 82.5 mm diameter cylindrical bore with a 6.35 mm  $\times$  3.17 mm key-way. The vertical cylindrical heater-well, which is an integral part of the steel extension piece, has a diameter of 76.2 mm and houses a 54 mm diameter 800 W resistive coil heater rated for a maximum operating temperature of 1200 °C in an oxidizing environment (100 mTorr vacuum). The choice of resistive coil heating is dictated by the desired temperature range as well as the heating rates it enables when compared with other commercially available resistive heating elements. The heater-head is attached to a vertical stem with over a 100 mm of axial reach, which allows the heater to be safely drawn-in and stored within the heater well prior to firing the gas-gun. Moreover, to enable elevated temperature oblique plate impact experiments, a full 360° of rotational freedom is provided to the heater head so as to align it parallel to an inclined flyer plate on the sabot.

A heat-resistant sabot is designed strategically to minimize heat transfer to the sabot body (by conduction) from the heated specimen plate end of the sabot, this is shown schematically in Fig. 3.2. Traditionally, sabots used in plate impact experiments are machined almost entirely from aluminum or Lexan; in the present application, however, precautions must be taken to prevent thermal expansion as well as thermal softening of the sabot so as to avoid seizure of the sabot in the gun barrel. The new sabot design comprises an aluminum cap adhered to an aluminum tube 200 mm in length and 82.5 mm in diameter using two-part 5-minute epoxy. The cap accommodates a sealing O-ring and an alignment key, which slides in the slotted keyway in the gun barrel to prevent rotation of the sabot during its acceleration down the gun barrel [8]. The length of the aluminum tube is strategically selected to enable impacts with tilts  $<0.3$  mrad, thus ensuring validity of one-dimensional wave theory in the interpretation of the experimental results [9]. In order to mitigate heat flow into the aluminum tube from the heated sample at the front of the sabot, a cylindrical tube fabricated from a low thermal conductivity and low thermal expansion material, e.g. fully-fired alumina silicate Lava rock, is utilized as an extension to the aluminum tube with the heated sample placed on a sample holder adhered to the Lava rock extension tube. The low thermal conductivity of the Lava rock tube helps to reduce heat loss from the heated sample plate to the sabot thus allowing the sample to quickly attain the desired test temperature, while the low thermal expansion of Lava rock prevents its interference with the precision gun barrel.

To demonstrate the feasibility of this approach, we conducted a series of three symmetric normal plate impact experiments at temperatures ranging from room at 650 °C on WC. Figure 3.3 shows the schematic of the experimental configuration. The experiments were conducted in the modified 82.5 mm bore single-stage gas gun facility at CWRU [10]. Prior to acceleration of the sabot, the sample (flyer plate) is heated by radiation to the desired test temperature using the specially designed resistive

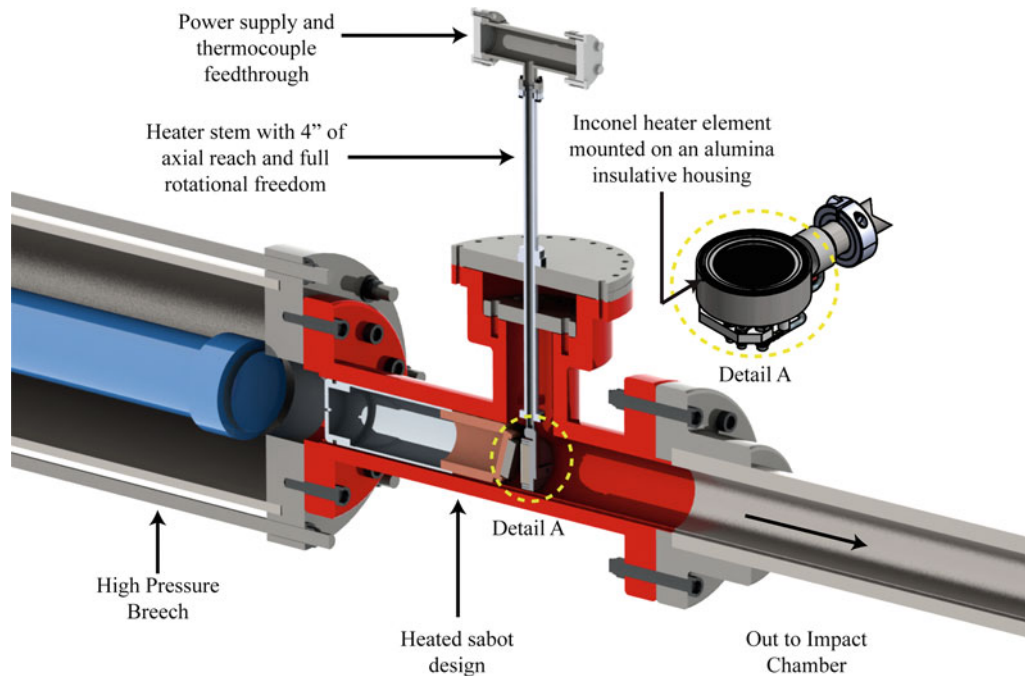


**Fig. 3.1** Shows a schematic of the breech-end heating system

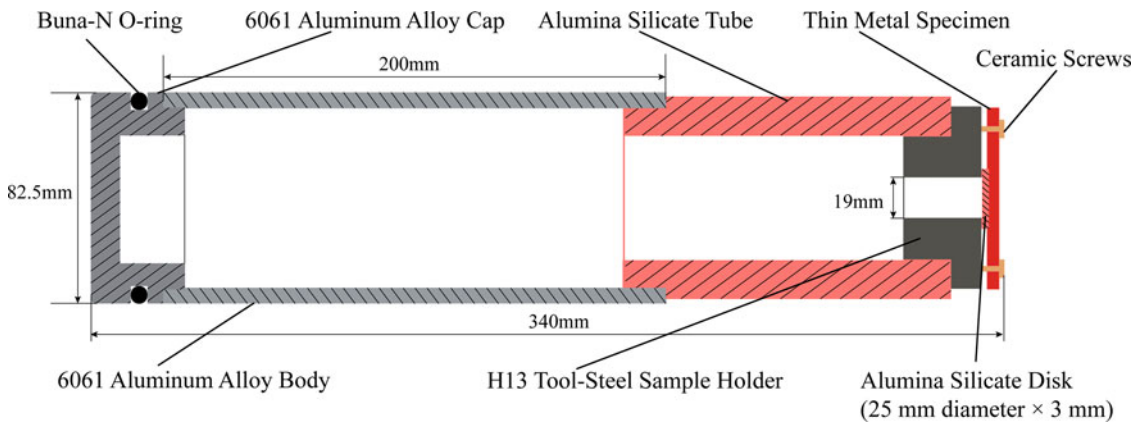


**Fig. 3.2** Shows a schematic of the sabot used in current experimental configuration. The alumina silicate tube helps mitigate heat flow from the heated thin metal specimen to the sabot body, thus minimizing the risk of seizure of the sabot within the gun-barrel due to possible thermal expansion of the sabot body

coil heater. The temperature of the sample is monitored continuously via a thermocouple probe attached to the sample. The impact is made to occur in a target chamber evacuated to a pressure less than 100 mTorr. Once the desired temperature is reached, the resistive coil heater is manually moved away from the path of the sabot and stored within the heater-well. Immediately following this step, the temperature displayed by the thermocouple is recorded, and the sabot carrying the flyer plate is accelerated down the gun barrel by means of compressed nitrogen gas to the desired impact velocity (which is approximately 100 m/s in the present experiments). The recorded temperature provides an estimate of the sample temperature at impact, while a custom laser amplitude-based velocity system is used to estimate the sabot velocity at impact. An in-house built fiber-optics-based NDI/TDI [11] is used to measure the particle displacement history at the free surface of the target plate.

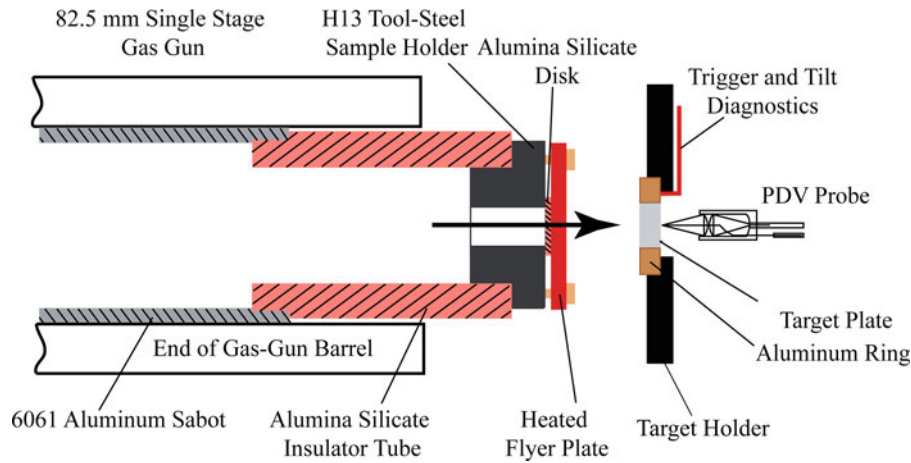


**Fig. 3.3** Schematic of the high temperature symmetric normal plate impact experiment. Here a heated flyer plate is carried by a custom heat-resistant sabot and is made to impact a stationary target plate

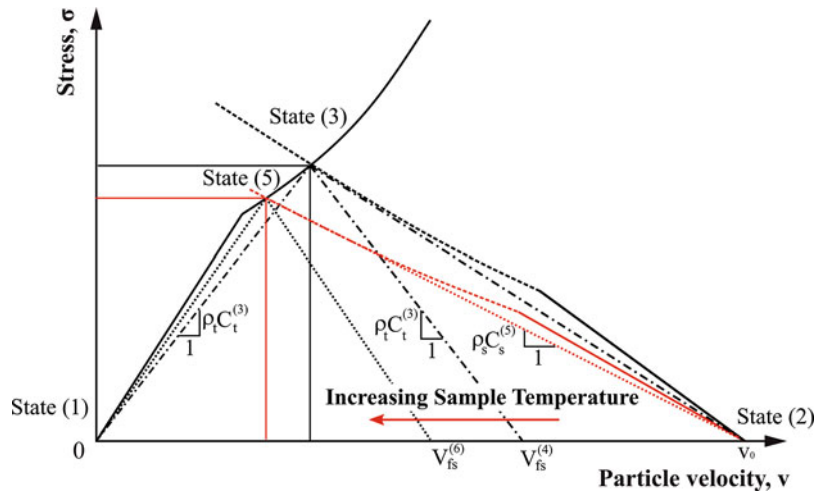


**Fig. 3.4** Shows the stress versus particle velocity diagram for a general elevated temperature normal plate impact experiment. The curve centered at origin details the locus of all stress states achievable for the isotropic target plate, whereas the curve originating at  $V_0$  details the locus of all states for the sample material at room temperature, moreover, the red curve intersecting  $V_0$  is meant to show the possible effect of increasing temperatures. Upon impact against a room temperature sample, the target plate moves from an un-loaded state (1) to a loaded state (3), whereas, if impact is made against a pre-heated sample, the target will move from state (1) to state (5), consequently, shifting the free surface particle velocity states from (4) to (6)

In the interpretation of the velocity trace we refer to the stress versus particle velocity (SV) diagram for a general case of a symmetric normal shock compression plate-impact experiment in which both the pre-heated flyer and the target plate can undergo elastic-plastic deformation at impact, this is shown in Fig. 3.4. The loci of all stress/particle velocity states for the target plate under uniaxial strain is represented by the black curve passing through the origin, while the loci of all stress/particle velocity states for the flyer is represented by the black curve intersecting the particle velocity axis at the projectile velocity. The red curve intersecting the particle velocity axis at the projectile velocity illustrates the possible effect of temperature on the locus of states for the flyer plate. For an impact against a room temperature flyer plate, at the flyer/target interface the target plate moves from an un-loaded state (1), to a loaded state (3), following the dash-dot line with a slope equal to the longitudinal impedance of the target plate material at state (3), while the flyer plate moves from an unloaded state (2) to a loaded state (3), following the line with a slope equal to the longitudinal impedance of the flyer plate at state (3). The intersection between these two lines reveal the maximum stress and velocity states achievable through impedance matching during this experiment at the sample/target interface. Moreover, the stress/particle velocity states at the flyer/target interface affect the particle velocity states at the free surface of the target plate, this shown as state (4). Impact against a flyer plate with a lower longitudinal impedance, would result in a change in achievable states at the sample/target interface

from (3) to (5), and consequently, at the free surface of the target from (4) to (6), thus, this shows how slight changes in the impedance of the flyer plate are detectable by monitoring the particle velocity at the free surface of the target plate.

Using a simple wave strain-rate independent longitudinal wave analysis, the compressive stress in the target interior can be related to the free surface particle velocity by using [5, 12–14].

$$\sigma_T(t^n) = \rho_T C_{LT} \frac{1}{1 + \frac{C_{LT}}{C^n}} V_{fs}(t^n) \quad (3.1)$$

where  $t^n$  is a discretized time interval represented as  $t^n = nh$ , where  $h$  is the inverse of the sampling rate of the oscilloscope ( $2.5 \times 10^{10}$  /s),  $t^n = t^n - L/C^n$  where  $L$  is the thickness of the target plate and  $C^n$  is an average stress dependent speed of plastic wave propagation in the target plate measured at the free surface at time  $t^n$ . The density and elastic longitudinal wave speed of the target plate are denoted by  $\rho_T$  and  $C_{LT}$ , respectively, and  $V_{fs}$  is the measured particle velocity at the free surface of the target plate. The strain,  $\varepsilon^n$ , and strain-rate,  $\dot{\varepsilon}^n$ , are given by

$$\varepsilon^n = \varepsilon^{n-1} + \frac{V_{fs}^n - V_{fs}^{n-1}}{C^n + C^{n-1}}, \quad (3.2)$$

and

$$\dot{\varepsilon}^n = \frac{\varepsilon^n - \varepsilon^{n-1}}{t^n - t^{n-1}}. \quad (3.3)$$

Additionally, from the measured free surface particle velocity corresponding to the velocity plateau (state (3)), the longitudinal acoustic impedance of the flyer (sample), can be estimate using

$$\rho_F C_F^{(3)} = \frac{\rho_T C_T^{(3)} V_{fs}^{(3)}}{\left(1 + \frac{C_T^{(3)}}{C_{LT}}\right) V_o - V_{fs}^{(3)}}. \quad (3.4)$$

### 3.3 Results and Discussion

Figure 3.5 shows the free surface particle velocity versus time record obtained from symmetric normal plate impact experiments on WC with varying initial flyer plate temperatures ranging from 23 to 650 °C. The profiles show three distinct regions: (1) an initial sharp linear rise in particle velocity after the arrival of the longitudinal wave at the free surface of the target plate, (2) a more moderate rise in particle velocity, followed by (3) a velocity plateau region. Region (1) is believed to be controlled by the elastic behavior of the material. The transition from region (1) to (2) is understood to represent the HEL of WC, which remains nearly constant at  $\sim 112$  m/s in the three experiments. The particle velocity profile in Region 2 is understood to be due to inelasticity (incipient plasticity) of the impacting plates, while the particle velocity level in the plateau region is dependent on the instantaneous longitudinal impedance of the flyer and target plates via Eq. (3.4).

Figure 3.6 shows estimates for the longitudinal impedance of the heated flyer plate, obtained by using Eq. (3.4), for the three cases. The results reveal a monotonic decrease in the shock impedance of WC with temperature. The overall trend fits well to a second order polynomial, and decreases by about 22% across temperature range of 23–650 °C.

To determine the stress versus strain response of WC, Regions (1) and (2) of the particle velocity trace are analyzed using Eqs. (3.1, 3.2, and 3.3). The results for the three cases are shown in Fig. 3.7. The lines centered at origin correspond the response of the material assuming linear elasticity, while the curve corresponds to the estimated elastic and plastic response. In all the three cases, the response of the WC target is essentially the same: a linear elastic regime up to approximately 6 GPa (strain-rates  $\sim 10^5$ /s), followed by a slight curve which deviates downwards from the elastic line. Since the development of incipient plasticity in the heated flyer and the target plates is understood to lower particle velocity in the flyer/target interface region, the strain rates achieved at the impact face is lowered accordingly.



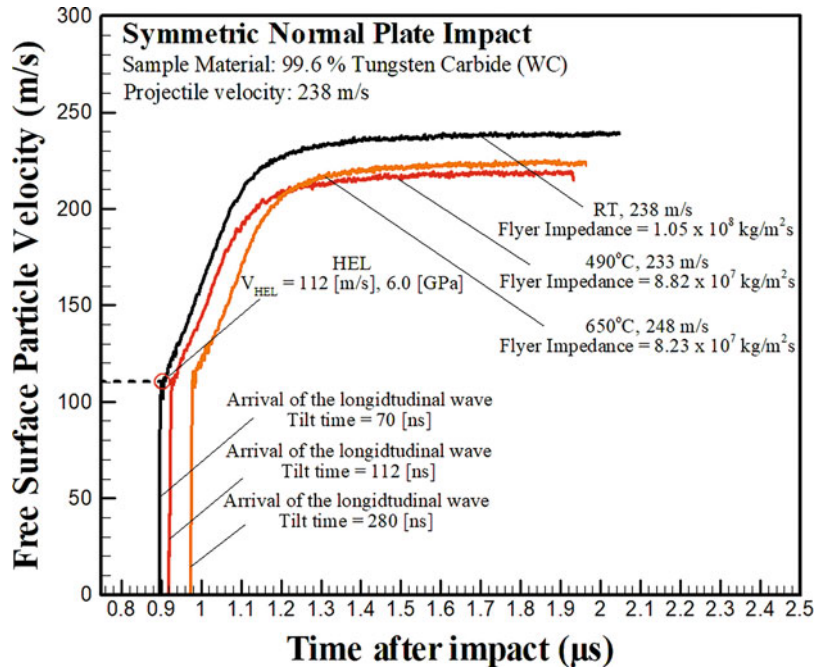


Fig. 3.5 Shows the particle velocity trace measured at the free surface of the target plate

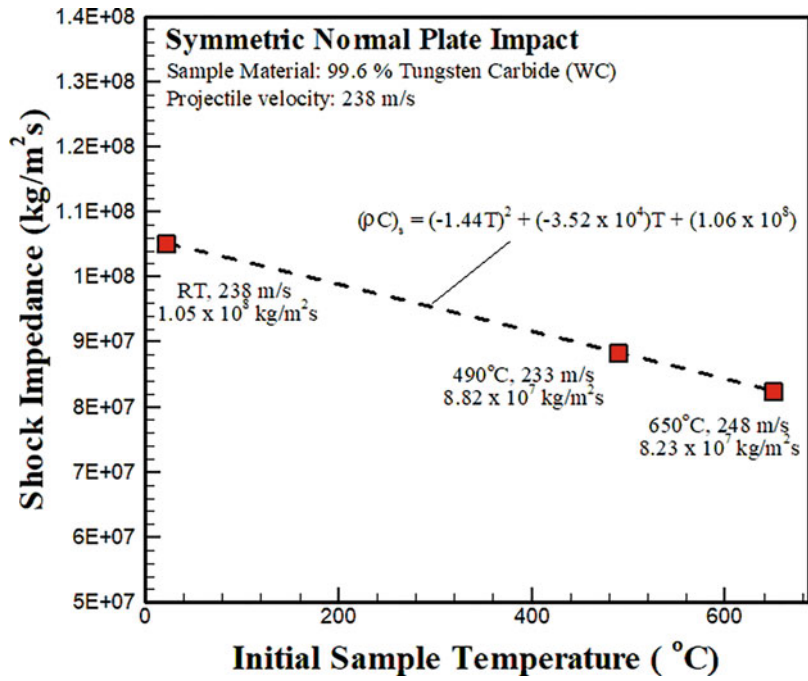
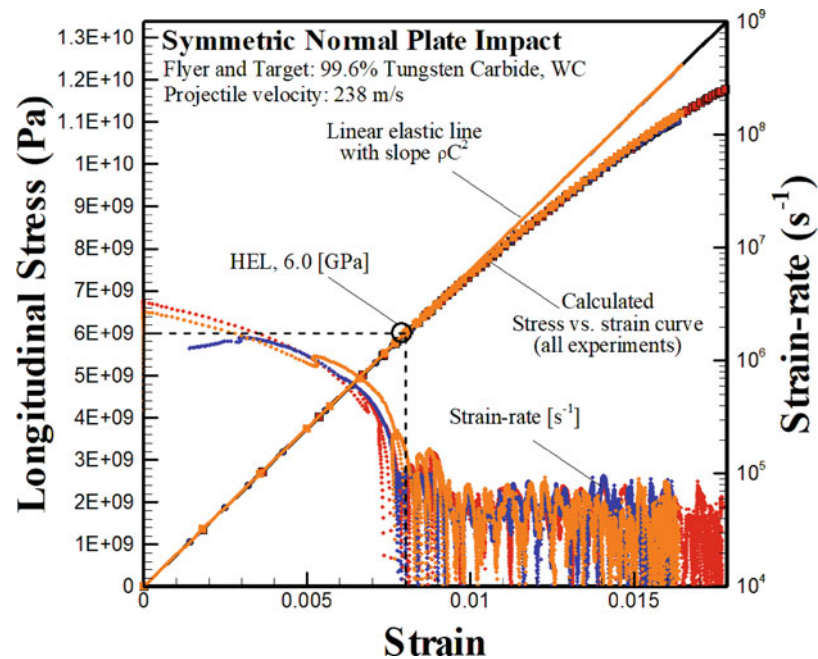


Fig. 3.6 Shows a gradual decrease in shock impedance with increasing flyer plate temperature

### 3.4 Summary

The paper presents a novel approach to conduct normal and/or combined pressure-shear plate impact experiments with initial sample temperatures up to 1000 °C. To enable this approach, custom adaptations are made to the breech-end of the single-stage gas-gun at Case Western Reserve University. The adaptations include a precision-machined steel extension piece, which is strategically designed to mate the existing gun-barrel and contains a vertical cylindrical heater-well and houses a resistive coil heater attached to a vertical stem with axial/rotational degrees of freedom. The assembly enables thin metal specimens



**Fig. 3.7** Shows the estimated stress versus strain response of the target plate under a symmetric normal plate impact resulting from applied axial loads of up to 12 GPa. The black line centered at origin shows an estimate of the material response assuming linear elasticity, while the red line shows the measured response. The plot clearly shows a deviation from the elastic regime at around 6 GPa corresponding to the Hugoniot elastic limit of WC

held at the front-end of a heat-resistant sabot to be heated uniformly across the diameter to the desired test temperatures prior to firing. Using this configuration, a series of three symmetric normal plate impact experiments are conducted on 99.6% WC (no binder) using a heated (room temperature to 650 °C) WC flyer plate and a room temperature WC target at impact velocities in the range 233–248 m/s. The measured free-surface particle velocity profiles are used to obtain the dynamic strength (HEL) of WC as well as the temperature-dependent longitudinal impedance of the WC flyer plate. The results indicate a dynamic strength of  $\sim 6$  GPa for the WC (at strain-rates of about  $10^5/s$ ), and a decreasing longitudinal impedance of the heated WC flyer with increasing temperatures up to 650 °C.

**Acknowledgment** The authors would like to acknowledge the financial support of the U.S. Department of Energy through the Stewardship Science Academic Alliance (DE-NA0001989 and DE-NA0002919).

## References

1. Prakash, V., Clifton, R.J.: Experimental and analytical investigation of dynamic fracture under conditions of plane strain. in *Fracture Mechanics: Twenty-Second Symposium* (1990)
2. Liou, N.-S., Okada, M., Prakash, V.: Formation of molten metal films during metal-on-metal slip under extreme interfacial conditions. *J. Mech. Phys. Solids*. **52**(9), 2025–2056 (2004)
3. Sunny, G., et al.: Effect of high strain rates on peak stress in a Zr-based bulk metallic glass. *J. Appl. Phys.* **104**(9), 093522 (2008)
4. Zaretsky, E., Kanel, G.I.: Effect of temperature, strain, and strain rate on the flow stress of aluminum under shock-wave compression. *J. Appl. Phys.* **112**(7), 073504 (2012)
5. Frutschy, K., Clifton, R.: High-temperature pressure-shear plate impact experiments using pure tungsten carbide impactors. *Exp. Mech.* **38**(2), 116–125 (1998)
6. Grunschel, S.E.: Pressure-shear plate impact experiments on high-purity aluminum at temperatures approaching melt. Doctoral Dissertation. Brown University (2009)
7. Dolan, D.H., et al.: Note: heated flyer-plate impact system. *Rev. Sci. Instrum.* **85**(7), 076102 (2014)
8. Yuan, F., Liou, N.-S., Prakash, V.: High-speed frictional slip at metal-on-metal interfaces. *Int. J. Plast.* **25**(4), 612–634 (2009)
9. Prakash, V.: Time-resolved friction with applications to high-speed machining: experimental observations. *Tribol. Trans.* **41**(2), 189–198 (1998)
10. Tsai, L., Prakash, V.: Structure of weak shock waves in 2-D layered material systems. *Int. J. Solids Struct.* **42**(2), 727–750 (2005)

11. Zuanetti, B., Wang, T., Prakash, V.: A compact fiber optics-based heterodyne combined normal and transverse displacement interferometer. *Rev. Sci. Instrum.* **88**(3), 033108 (2017)
12. Zuanetti, B., Wang, T., Prakash, V.: Mechanical response of 99.999% purity aluminum under dynamic uniaxial strain and near melting temperatures. *Int. J. Impact. Eng.* **113**, 180–190 (2018)
13. Wang, T., Zuanetti, B., Prakash, V.: Shock response of commercial purity polycrystalline magnesium under uniaxial strain at elevated temperatures. *J. Dyn. Behav. Mater.* **3**(4), 497–509 (2017)
14. Okada, M., et al.: Tribology of high-speed metal-on-metal sliding at near-melt and fully-melt interfacial temperatures. *Wear.* **249**(8), 672–686 (2001)